J Electr Eng Technol.2017; 12(1): 110-116
http://dx.doi.org/10.5370/JEET.2017.12.1.110

ISSN(Print) 1975-0102
ISSN(Online) 2093-7423

A Maximum Power Control of IPMSM with Real-time Parameter Identification

Hyunwoo Jun*, Hanwoong Ahn*, Hyungwoo Lee, Sungchul Go*** and Ju Lee†**

Abstract – This paper proposed a new real-time parameter tracking algorithm. Unlike the convenience algorithms, the proposed real-time parameter tracking algorithm can estimate parameters through three-phase voltage and electric current without coordination transformation, and does not need information on magnetic flux. Therefore, it can estimate parameters regardless of the change according to operation point and cross-saturation effect. In addition, as the quasi-real-time parameter tracking technique can estimate parameters through the four fundamental arithmetic operations instead of complicated algorithms such as numerical value analysis technique and observer design, it can be applied to low-performance DSP. In this paper, a new real-time parameter tracking algorithm is derived from three phase equation. The validity and usefulness of the proposed inductance estimation technique is verified by simulation and experimental results.

Keywords: Real-time parameter tracking algorithm, Inductance identification, Maximum power control, IPMSM

1. Introduction

To accommodate many passengers and move at a high speed, a train requires a traction motor with high-density output within limited physical dimensions. A traction motor, likewise, is constantly becoming smaller in size, as well as is requiring a higher-efficiency motor. Thus, the interior permanent magnet synchronous motor (IPMSM) is increasingly being adjusted as a traction motor for trains, since the IPMSM is generated as magnetic and reluctance torque becomes overlapped, it can produce torque far higher than other motors did [1,2].

However, if the correct parameter of IPMSM cannot be predicted or estimated, problems of reduced output, low-efficient operation, and even out-of-synchronization can occur. Also, since IPMSM has a severe local self-saturation, motor parameters such as resistance (R) and inductance (L_d, L_q) change nonlinearly by all kinds of conditions including electric current and phase angle [3]. Especially, as the change aspect of inductance (L_d, L_q) varies irregularly depending on the capacity, shape, and operating characteristics of motor, the incorrect estimation of parameter reduces motor operation performance [4]. Thus, the correct estimation of inductance that changes in real-time is a necessary element for designing a controller and guaranteeing an excellent control performance.

† Corresponding Author: Dept. of Electrical Engineering, Hanyang University, Korea. (julee@hanyang.ac.kr)
* Dept. of Electrical Engineering, Hanyang University, Korea. ({jhwinc, zemlja}@naver.com)
** Dept. of Railway Vehicle System Engineering, Korea National University of Transportation, Korea. (krhwlee@ut.ac.kr)
*** Mechatronics R&D Center, Samsung Electronics Co., Korea. (sc.go@samsung.com)
Received: February 3, 2016; Accepted: June 8, 2016

The estimation methods can be divided into two: the offline parameter estimation methods which are to estimate through test-operation, and the online parameter estimation methods which estimates during operation. The offline parameter estimation methods have the merit of easily being implemented thanks to its simple algorithm. Nonetheless, they also have disadvantages: need for additional equipment; and measurement error being caused as compared with the actual operation due to the estimation conducted from a single point.

Meanwhile, the online parameter estimation is suitable for applications that have various operation ranges, because it is estimation during operation. However, its algorithm is fairly complex, implementation is difficult, and it often requires high-performance DSP.

The offline parameter estimation techniques can be classified into the estimation methods which do the estimation at standstill conditions and ones implemented at operating conditions. The estimation methods in the standstill conditions include the DC current decay test and AC standstill methods [5, 6]. On the other hand, the estimation methods for the operating conditions include the vector-controlled method and generator test [7, 8].

The online parameter estimation techniques are introduced as the model reference adaptive control techniques, observer-based techniques, extended kalman filter based Techniques, and neural network techniques [9-12].

Previous technologies have the disadvantages of failing to consider uneven operating conditions of a motor, or requiring complex calculation. Additionally, the magnetic flux are required for the parameter estimation of a permanent magnet synchronous motor; and these elements can change due to the motor's temperature or magnetic

saturation [13]. Thus, it is difficult to exactly estimate a parameter.

This paper deals with conducting exact maximum power of IPMSM through suggesting estimation methods for the inductance (L_d, L_q) of IPMSM without considering the magnetic flux.

2. IPMSM Equivalent Circuit

For vector control of IPMSM, the three-phase voltage equation formula of IPMSM was calculated through Clarke transformation and Park transformation in order, which obtained d-q axes voltage equation as in (1) [14].

$$\begin{bmatrix} v_{ds}^r \\ v_{qs}^r \end{bmatrix} = \begin{bmatrix} R_a & -\omega L_q \\ \omega L_d & R_a \end{bmatrix} \begin{bmatrix} i_{ds}^r \\ i_{qs}^r \end{bmatrix} + \begin{bmatrix} 0 \\ \omega_e \Psi_a \end{bmatrix} \tag{1}$$

The torque equation of IPMSM is given as follows

$$T_e = \frac{3}{2}\frac{P}{2}\left\{\Phi_a i_q + \left(L_d - L_q\right) i_d i_q\right\} \tag{2}$$

Magnetic flux could obtain data by the B_r value of permanent magnet, and stator resistance could be measured easily through DC test. However, L_d and L_q changed according to the d- and q-axis current, and their characteristics change due to the saturation of core. Thus, it is necessary to develop technology that can accurately estimate L_d and L_q. Especially when the inductance while controlling torque can be estimated, exact calculation of actual torque is possible, resulting in substantial reduction of the measurement error between command and actual torque, so that torque can be controlled with high efficiency and good performance.

3. Maximum Power Control of IPMSM

A maximum torque-per-ampere (MTPA) and field weakening control are performed to implement the maximum power control of IPMSM. While under the base speed, it conducts control of the MTPA, which generates the highest torque for the identical armature current [15,16]. As in Fig. 1(a), the IPMSM always exists with the highest level current topology for the identical current. Therefore, if the current phase angle β in (2) is partially differentiated, the MTPA optimal operating line can be derived as follows

$$i_d = \frac{\Phi_a}{4\left(L_q - L_d\right)} - \sqrt{\frac{\Phi_a^2}{16\left(L_q - L_d\right)^2} + \frac{I_a^2}{2}} \tag{3}$$

$$i_q = \sqrt{I_a^2 - i_d^2} \tag{4}$$

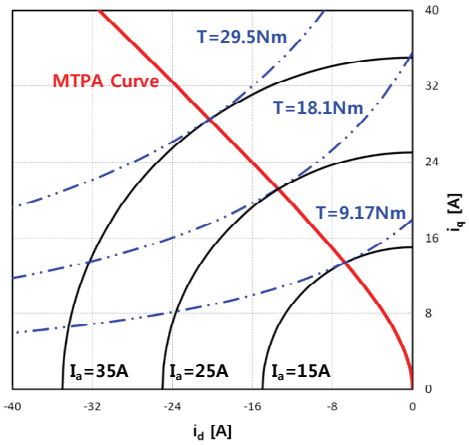

(a) MTPA

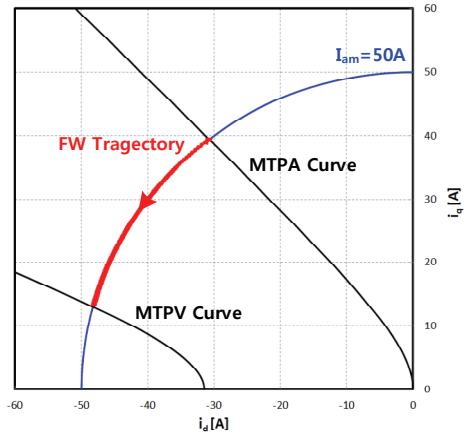

(b) Field Weakening

Fig. 1. Current Vector Locus of the MTPA and FW Control

When the motor reaches the base speed, the voltage limit comes into effect, so no more acceleration through the MTPA control is possible. Hence, in order to have a wider speed range, the field weakening (FW) control is conducted with the allowing of the negative d-axis current. Fig. 1(b) shows the trajectory of the FW control. The operating point of the FW control moves along the constant current circle, and the intersection point of the constant voltage ellipse and constant current source can yield the following results.

$$i_d = \frac{\Phi_a L_d - \sqrt{\left(\Phi_a L_q\right)^2 + \left(L_q^2 - L_d^2\right)\left\{\left(L_q I_{am}\right)^2 - \left(\frac{V_{om}}{\omega}\right)^2\right\}}}{L_q^2 - L_d^2} \tag{5}$$

$$i_q = \sqrt{I_{am}^2 - i_d^2} \tag{6}$$

As in (3) to (6), the information of d- and q-axis inductances is required to conduct the MTPA and FW control. Inaccurate d-and q-axis inductances cannot accurately determine operating points, and this becomes a

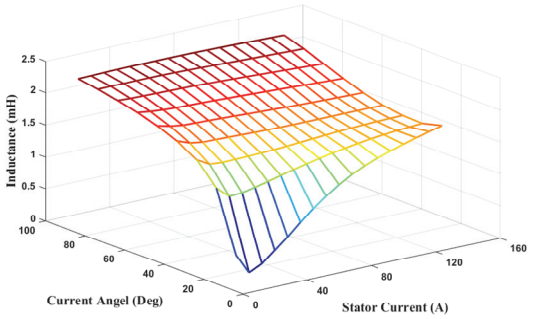

(a) d-axis inductance

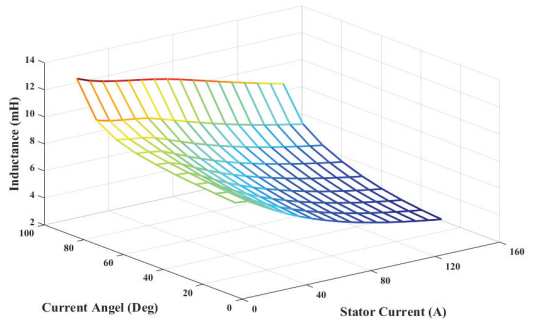

(b) q-axis inductance

Fig. 2. d- and q-axis Inductances following Stator Current and Current Phase Angle

degradation factor for the motor's performance.

Fig. 2 is the calculation of d- and q-axis inductances through FEM following the current phase angle and stator current of the IPMSM The d- and q-axis inductances change by the current phase angle and stator current as seen in the Fig. 2. Therefore, in order to maximum power control with high performance, the real-time information of the d- and q- axis inductances is required.

4. Quasi-realtime Parameter Tracking

The conventional parameter estimation of IPMSM was carried out mostly on d and q axes. However, this paper proposed a technique that can estimate L_d and L_q from a, b, c axes instead of d, q axes, in order to have an approach from a physical perspective. The online inductance estimation suggested by this paper can be drawn through the following three steps.

4.1 Calculation of No-load line-line Back-EMF

The three-phase voltage formula for the IPMSM is as follows.

$$\mathbf{v}_{\mathbf{abc}} = R_a \mathbf{i}_{\mathbf{abc}} + \mathbf{L}_{\mathbf{s}} \frac{d\mathbf{i}_{\mathbf{abc}}}{dt} + \mathbf{i}_{\mathbf{abc}} \frac{d\mathbf{L}_{\mathbf{s}}}{dt} + \mathbf{e}_{\mathbf{abc}} \tag{7}$$

Here, v_{abc}, i_{abc}, L_s, e_{abc} are vectors that represent the physical quantity of the phase a, b, and c. Calculation of no-load line-line back EMF from the phase a, b, and c voltage equation in (7) can be represented as follows.

$$V_{ab} = R_a i_{ab} + L_N \frac{di_{ab}}{dt} + \alpha_{ab} L_M + \beta_{ab} \tag{8}$$

$$V_{bc} = R_a i_{bc} + L_N \frac{di_{bc}}{dt} + \alpha_{bc} L_M + \beta_{bc} \tag{9}$$

$$V_{ca} = R_a i_{ca} + L_N \frac{di_{ca}}{dt} + \alpha_{ca} L_M + \beta_{ca} \tag{10}$$

Here, $L_N=L_{ls}+3/2L_A$, $L_M=L_B$. The L_{ls} indicates leakage inductance, L_A the average self-inductance, and L_B the amplitude of self-inductance. Each coefficient is the same as in (11) ~ (16).

$$\alpha_{ab} = \sqrt{3}\left(\sin\left(2\theta_r - \frac{\pi}{3}\right)\frac{di_a}{dt} + \sin\left(2\theta_r - \pi\right)\frac{di_b}{dt} + \sin\left(2\theta_r + \frac{\pi}{3}\right)\frac{di_c}{dt}\right) + 2\sqrt{3}\omega_r\left(\cos\left(2\theta_r - \frac{\pi}{3}\right)\cdot i_a + \cos\left(2\theta_r - \pi\right) i_b + \cos\left(2\theta_r + \frac{\pi}{3}\right) i_c\right) \tag{11}$$

$$\alpha_{bc} = -\sqrt{3}\left(\sin 2\theta_r \cdot \frac{di_a}{dt} + \sin\left(2\theta_r - \frac{2}{3}\pi\right)\frac{di_b}{dt} + \sin\left(2\theta_r + \frac{2}{3}\pi\right)\frac{di_c}{dt}\right) + 2\sqrt{3}\omega_r\left(-\cos 2\theta_r \cdot i_a - \cos\left(2\theta_r - \frac{2}{3}\pi\right) i_b - \cos\left(2\theta_r + \frac{2}{3}\pi\right) i_c\right) \tag{12}$$

$$\alpha_{ca} = \sqrt{3}\left(\sin\left(2\theta_r + \frac{1}{3}\pi\right)\frac{di_a}{dt} + \sin\left(2\theta_r - \frac{1}{3}\pi\right)\frac{di_b}{dt} + \sin\left(2\theta_r + \pi\right)\frac{di_c}{dt}\right) + 2\sqrt{3}\omega_r\left(\cos\left(2\theta_r + \frac{\pi}{3}\right)\cdot i_a + \cos\left(2\theta_r - \frac{\pi}{3}\right) i_b + \cos\left(2\theta_r + \pi\right) i_c\right) \tag{13}$$

$$\beta_{ab} = -\sqrt{3}\omega_r \phi_f \cos\left(\theta_r - \frac{\pi}{3}\right) \tag{14}$$

$$\beta_{bc} = \sqrt{3}\omega_r \phi_f \cos\left(\theta_r\right) \tag{15}$$

$$\beta_{ca} = -\sqrt{3}\omega_r \phi_f \cos\left(\theta_r + \frac{\pi}{3}\right) \tag{16}$$

4.2 Elimination of magnetic flux

The three-phase no-load line-line back-EMF Eqs. (8)~(10) all contain magnetic flux elements. If β_{ab}/β_{bc}, β_{bc}/β_{ca}, and β_{ca}/β_{ab} are calculated for each no-load line-line back-EMF in order to eliminate magnetic flux, an equation which is unrelated to magnetic flux can be derived.

$$\frac{\beta_{ab}}{\beta_{bc}} = \frac{-\sqrt{3}\cos\left(\theta - \frac{\pi}{3}\right)}{\sqrt{3}\cos\theta} = \frac{V_{ab} - R_a i_{ab} - L_N \frac{di_{ab}}{dt} - \alpha_{ab} L_M}{V_{bc} - R_a i_{bc} - L_N \frac{di_{bc}}{dt} - \alpha_{bc} L_M} \tag{17}$$

$$\frac{\beta_{bc}}{\beta_{ca}} = \frac{\sqrt{3}\cos\theta}{-\sqrt{3}\cos\left(\theta+\frac{\pi}{3}\right)} = \frac{V_{bc} - R_a i_{bc} - L_N \frac{di_{bc}}{dt} - \alpha_{bc} L_M}{V_{ca} - R_a i_{ca} - L_N \frac{di_{ca}}{dt} - \alpha_{ca} L_M} \quad (18)$$

$$\frac{\beta_{ca}}{\beta_{ab}} = \frac{-\sqrt{3}\cos\left(\theta+\frac{\pi}{3}\right)}{-\sqrt{3}\cos\left(\theta-\frac{\pi}{3}\right)} = \frac{V_{ca} - R_a i_{ca} - L_N \frac{di_{ca}}{dt} - \alpha_{ca} L_M}{V_{ab} - R_a i_{ab} - L_{ls} \frac{di_{ab}}{dt} - \alpha_{ab} L_M} \quad (19)$$

4.3 Estimation of L_d and L_q

L_N and L_M are derived when (20), (21) is solved.

$$L_d = L_{ls} + \frac{3}{2}(L_A - L_B) = L_N - \frac{3}{2} L_M \quad (20)$$

$$L_q = L_{ls} + \frac{3}{2}(L_A + L_B) = L_N + \frac{3}{2} L_M \quad (21)$$

Here, the feasibility of problem should be guaranteed in order to be a solution. This feasibility can be satisfied by choosing appropriate initial condition. The initial condition is assumed to be the rating condition of a motor.

Fig. 3 represents the speed control block diagram of the IPMSM through the parameter estimation method which this paper has suggested. The initial condition is entered into the parameter estimator to estimate the inductance of

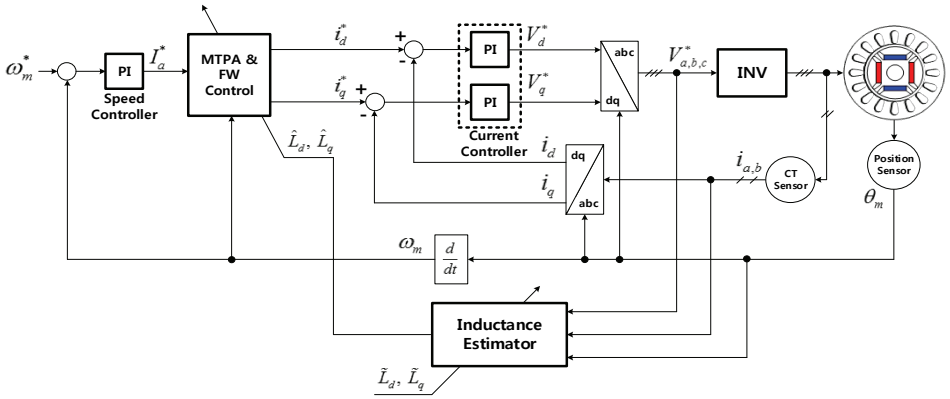

Fig. 3. Speed controller based on maximum torque-per-ampere and field weakening control with inductance estimator

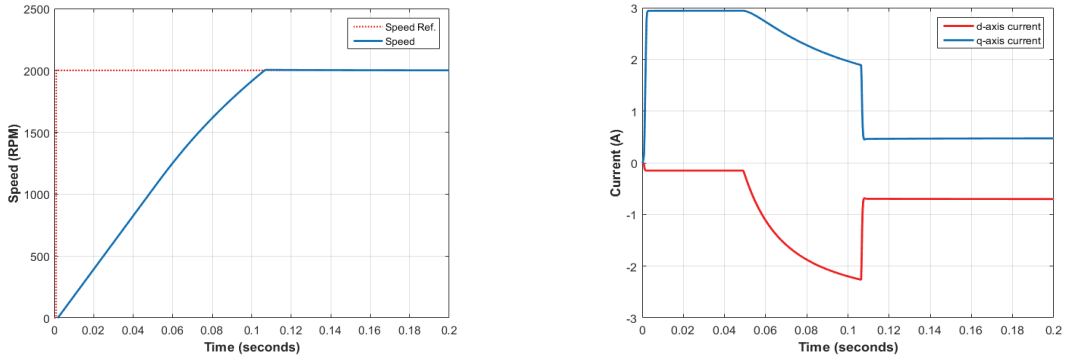

(a) Motor speed

(b) d, q-axis current

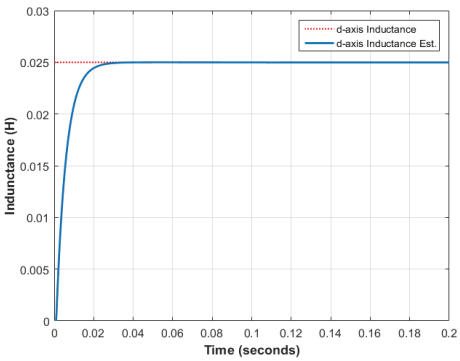

(c) d-axis inductance

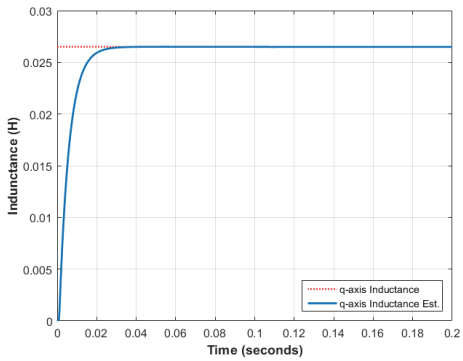

(d) q-axis inductance

Fig. 4. Simulation Result of Quasi-realtime Parameter Tracking Method

the IPMSM. The estimated inductance determines the operating points during MTPA and FW control.

5. Simulation Results

The proposed inductance estimation method is simulated by MATLAB/Simulink. Specification details for the motor are in Table 1. The speed reference of 2,000 RPM is entered which is above the base speed, so that inductance estimation can be tested during the MTPA and FW control of the IPMSM. Fig. 4 shows the simulation result of the test motor. In Fig. 4(a), the motor speed converging according to the speed reference can be identified. Fig. 4(b) shows the d- and q-axis current. d- and q-axis current holds a constant value during the MTPA control, and as it rises above the base speed, the d-axis current is increased while the q-axis current decreases due to the FW control. Fig. 4(c) and (d) show the d- and q-axis inductances at the moment. The actual value is precisely estimated regardless of the motor's control mode. Fig. 5 exhibits the simulation result which included the change of inductance values under real operational condition. It shows that the estimated value accurately follows the actual value when inductance changes.

Table 1. The Specifications of IPMSM

Parameter	Value	Unit
N_p	8	
V_{dc}	100	V
I_{am}	3	A
R_a	2.85	Ohm
T_{max}	1.54	Nm
Φ_a	0.087	Wb
L_d	25	mH
L_q	26.5	mH
J_m	$5.7 \cdot 10^{-5}$	kg· m^2

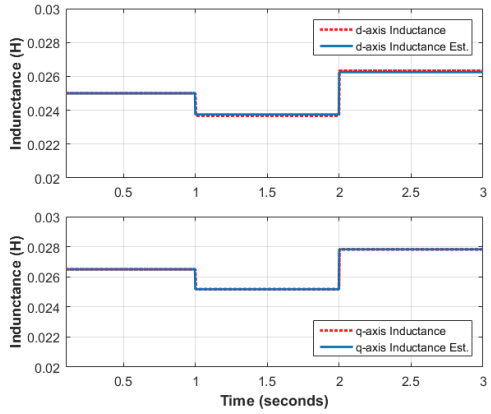

(a) Ramp Response

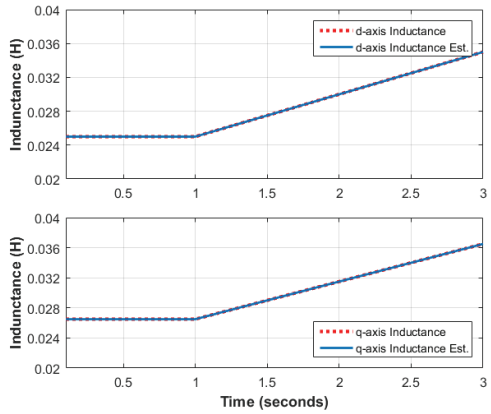

(b) Step Response

Fig. 5. Simulation result in accordance with the variation of inductance

6. Experiment

In order to verify the performance of the proposed algorithm, the experiment is performed. The experimental test setup is shown in Fig. 6. DSP TMS320F28335 is used for IPMSM control and load torque is generated by dynamometer.

Fig. 8 shows the inductance estimation results when the rotational speed of the motor at 1,000 [RPM]. As shown in Fig. 7, phase currents are applied to the rated current. In

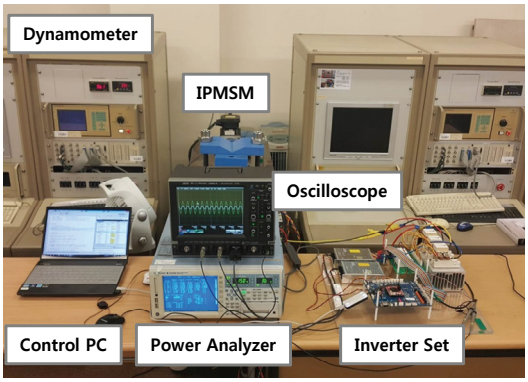

Fig. 6. Experimental setup

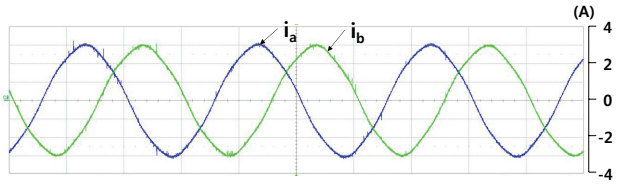

Fig. 7. a, b phase current for inductance estimation

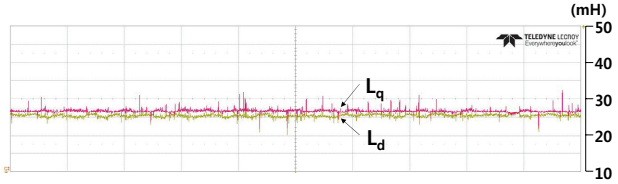

Fig. 8. Inductance estimation results

Fig.8, yellow line represents d-axis inductance and red line indicates q-axis inductance. The results of the experiment, d-axis inductance is 25 [mH] and d-axis inductance is shown in 26.5 [mH]. It can be confirmed that proposed inductance estimation results is same with the actual value of the Table 1.

7. Conclusion

The inductance of the IPMSM is an essential parameter to control high-performance motors while, for instance, torque, speed, or senseless controls. This newly developed estimation method takes an approach from the physics view, estimating the L_d and L_q from the axis a, b, and c. Further, a equation has been derived, which is not affected by the non-linearity of magnetic flux, and thus accuracy has been enhanced.

The proposed inductance estimation algorithm was tested through the MATLAB/Simulink. In all speed ranges, the inductance estimation was precisely identified. Also, even when the inductance changed, it followed without measurement error, which verified the effectiveness of the proposed algorithm. Also, the validity of the proposed inductance estimation technique is confirmed throughout the experimental results.

Acknowledgements

This work was supported by the National Research Foundation of Korea(NRF) grant funded by the Korea government(Ministry of Science, ICT & Future Planning) (No. 2016R1A2A1A05005392 and 2016R1A2B4009675).

References

[1] S. F. Zhao, X. Y. Huang, Y. F. Fang, and J. Li, "A Control Scheme for a High Speed Railway Traction System Base on High Power PMSM", 2015 6th Int. Conf. Power Electron. Syst. Appl., pp. 1-8, Dec. 2015.

[2] C. B. Park, B. S. Lee, and H. W. Lee, "Performance Comparison of the Railway Traction IPM Motors between Concentrated Winding and Distributed Winding", J. Electr. Eng. Technol., Vol. 8, No. 1, pp. 118-123, Jan. 2013.

[3] K. D. Lee, J. Lee, and H. W. Lee, "Inductance Calculation of Flux Concentrating Permanent Magnet Motor through Nonlinear Magnetic Equivalent Circuit", IEEE Trans. Magnetics, Vol. 51, No. 11, Nov. 2015.

[4] W. H. Kim, M. J. Kim, K. D. Lee, J. J. Lee, J. H. Han, T. C. Jeong, S. Y. Cho, and J. Lee, "Inductance Calculation in IPMSM Considering Magnetic Saturation", IEEE Trans. Magnetics, Vol. 50, No. 1, Jan. 2014.

[5] E. S. Boje, J. C. Balda, R. G. Harley, and R. C. Beck, "Time-domain Identification of Synchronous Machine Parameters from Simple Standstill Test", IEEE Trans. Energy Convers., Vol. 5, No. 1, pp. 164-175, Mar. 1990.

[6] Rukmi Dutta and M. F. Rahman, "A Comparative Analysis of Two Test Methods of Measuring d - and q -Axes Inductances of Interior Permanent-Magnet Machine", IEEE Trans. Magnetics. Vol. 42, No. 11, pp. 3712-3718, Nov. 2006,

[7] Khwaja M. Rahman, Silva Hiti "Identification of Machine Parameters of a Synchronous Motor", IEEE Trans. Ind. Appl, Vol. 41, No. 2, pp. 557-565, Mar./ Apr. 2005.

[8] T. Senjyu, N. Urasaki, T. Simabukuro and K. Uezato, "Using on-line parameter estimation to improve efficiency of IPM machine drives", in Proc. IEEE PESC, Vol. 2, pp. 815-820, Jun. 2002.

[9] T. Boileau, N. Leboeuf, B. Nahid-mobarakeh, and F. Meibody-Tabar, "Online Identification of PMSM Parameters: Parameter Identifiability and Estimator Comparative Study", IEEE Trans. Ind. Appl., Vol. 47, No. 4, pp. 1944-1957, Jul./Aug. 2011.

[10] M. A. Hamida, J. D. Leon, A. Glumineau, and R. Boisliveau, "An Adaptive Interconnected Observer for Sensorless Control of PM Synchronous Motors with Online Parameter Identification", IEEE Trans. Ind. Electron., Vol. 60, No. 2, pp. 739-748, Feb. 2013.

[11] S. Wang, S. Shi, C. Chen, G. Yang, and Z. Qu, "Identification of PMSM based on EKF and Elman Neural Network" in Proc. ICAL, pp. 1459-1463, Aug. 2009.

[12] H. W. Sim, J. S. Lee, and K. B. Lee, "On-line Parameter Estimation of Interior Permanent Magnet Synchronous Motor using an Extended Kalman Filter", J. Electr. Eng. Technol., Vol. 9, No. 2, pp. 600-608, Mar. 2013.

[13] A. Yoo, and S. K. Sul, "Design of Flux Observer Robust to Interior Permanent-Magnet Synchronous Motor Flux Variation", IEEE Trans. Ind. Appl., Vol. 45, No. 5, pp. 1670-1677, Sep./Oct. 2011.

[14] J. F. Gieras, *Permanent Magnet Motor Technology*, 3rd ed. CRC Press, 2009.

[15] Thomas M. Jahns, Gerald B. Kliman, and Tomas W. Neumann, "Interior Permanent-Magnet Synchronous Motors for Adjustable-Speed Drives", IEEE Trans. Ind. Appl., Vol. IA-22, No. 4, pp. 738-747, Jul. 1986.

[16] B. K. Bose, "A high-performance inverter-fed drive system of an interior permanent magnet synchronous machine", IEEE Trans. Ind. Appl., Vol. 24, No. 6, pp. 987-997, Nov./Dec. 1988.

Hyunwoo Jun He received his B.S. and M.S. degrees in Electrical Engineering from Hanyang University, Seoul, Korea in 2012 and 2014, respectively. Since 2014, he has been pursuing the Ph.D. degree at the Department of Electrical Engineering, Hanyang University. His research interests include design, analysis, testing and control of motor/generator; power conversion systems; and applications of motor drive

Hanwoong Ahn He received his B.S. and M.S. degrees in Electrical Engineering from Hanyang University, Seoul, Korea in 2010 and 2012, respectively. Since 2012, he has been pursuing the Ph.D. degree at the Department of Electrical Engineering, Hanyang University. His research interests include design, analysis, testing and control of motor/generator; power conversion systems; and appli-cations of motor drive.

Hyungwoo Lee He received his M.S. degree from Hanyang University, Seoul, Korea, in 2000, and his Ph.D. from Texas A&M University, College Station, TX, in 2003, both in Electrical Engineering. He joined Korea National University of Transportation as professor of the department of Railway Vehicle System Engineering in March 2013. His research interests include motor design, analysis of motor / generator; and applications of motor drive, such as Maglev trains, conventional railway propulsion systems, and modern renewable energy systems.

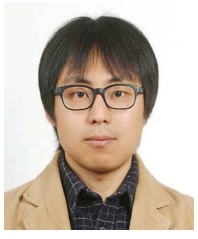

Sungchul Go He received his B.S., M.S. and Ph.D. degrees in Electrical Engineering from Hanyang University, Seoul, Korea in 2004, 2006 and 2010 respectively. He is now working in Samsung Electronics Co. His research interests include design, analysis, testing and control of motor/generator; power conversion systems; and applications of motor drive, such as electric vehicles, high-speed maglev train and renewable energy systems.

Ju Lee He received his M.S. degree from Hanyang University, Seoul, South Korea, in 1988, and his Ph.D. from Kyusyu University, Japan in 1997, both in Electrical Engineering, He joined Hanyang University in September, 1997 and is currently a Professor of the Division of Electrical and Biomedical Engineering. His main research interests include electric machinery and its drives, electromagnetic field analysis, new transformation systems such as hybrid electric vehicles (HEV), and high-speed electric trains and standardization. He is a member of the IEEE Industry Applications Society, Magnetics Society, and Power Electronics Society.